Technical Notes

TECHNICAL NOTES are short manuscripts describing new developments or important results of a preliminary nature. These Notes cannot exceed 6 manuscript pages and 3 figures; a page of text may be substituted for a figure and vice versa. After informal review by the editors, they may be published within a few months of the date of receipt. Style requirements are the same as for regular contributions (see inside back cover).

J80-189

Large Incidence Hypersonic Similitude and Oscillating Nonplanar Wedges

20009
20017

Kunal Ghosh* and Binoy Krishna Mistry†
Indian Institute of Technology, Kanpur, India

Introduction

SYCHEV'S[1] high-incidence hypersonic similitude is applicable to a wing provided it has an extremely small span in addition to small thickness. The unsteady infinite span case has been analyzed, but mostly for small flow deflections. The piston theory of Lighthill[2] neglects effects of secondary wave reflection. Appleton[3] (see Orlik-Rückemann[4] for some corrections) and McIntosh[5] have included these effects. Hui's[6] theory is valid for wedges of arbitrary thickness oscillating with small amplitude provided the bow shock remains attached. Ericsson's[7] theory covers viscous and elastic effects for airfoils with large flow deflection. Orlik-Rückemann[8] has included viscous effect, and Mandl[9] has addressed small surface curvature effect for oscillating thin wedges. Ghosh's[10] similitude and piston theory for the infinite span case with large flow deflection is recounted in this paper; it is valid for airfoils with planar or nonplanar surfaces, whereas Hui's[6] theory is for plane wedges. Ghosh's[10] piston theory has been applied to nonplanar cases, both steady and unsteady. The effect of viscosity and secondary wave reflection has not been included.

Analysis

Figure 1a shows an airfoil with attached bow shock, oscillating with small amplitude and frequency, having its windward nonplanar surface at an arbitrary incidence. The surface departs from $y=0$ plane by a small amount. The x axis is coincident with the chord of the windward surface in its mean position, and the lee surface pressure is considered negligible. The angle between the x axis and bow shock at leading edge is ϕ, which is a small quantity for hypersonic flow for incidences away from shock detachment. For the purpose of order-of-magnitude analysis, the windward surface is assumed planar so that $\phi=\beta-\alpha$, where β is the shock wave angle. From oblique shock relations, for large M_∞ and r (sp. heat ratio) $=1.4$, $M_2^2\sin^2\phi \doteq 0.143$, or

$$\sin^{-1}(1/M_2) \doteq \sin^{-1}2.64\phi \doteq 2.64\phi \ldots \qquad (1)$$

Therefore, δ, inclination of the characteristics behind the shock, is $0(\phi)$. The perturbation velocities in y and x directions are $q_y=0(U_\infty\sin\alpha)$ and $q_x=0(\phi U_\infty\sin\alpha)$. This suggests the transformations: $q_x=\phi q_x'$ and $x=\phi^{-1}x'$. However, for large ϕ, $\delta=0(\phi)$ is no longer valid, and the second transformation is not appropriate. For validity of this theory, $\phi\leq 0.175$ rad $=10$ deg. This implies, from Eq. (1), that the lower limit for M_2 is around 2.5. An analysis follows resembling the small disturbance theory and, therefore, is omitted here. A similitude where flow equations reduce to one-dimensional unsteady form is obtained, and hence, the piston analogy. The error in this theory is of $0(\phi^2)$. The nonplanar windward surface may depart from $y=0$ plane as much as in the case of corresponding compression surface in hypersonic small disturbance theory in which the condition $M_2\geq 2.5$ is also implicit since the characteristics are required to be at small inclinations. Therefore, the present similitude includes the two-dimensional small disturbance similitude for the compression side.

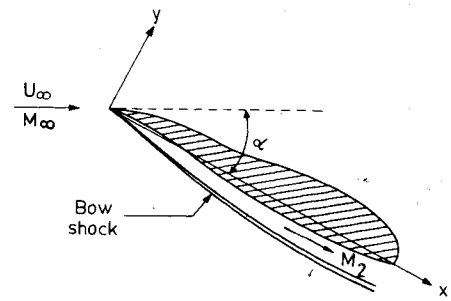

Fig. 1 a) Coordinate system.

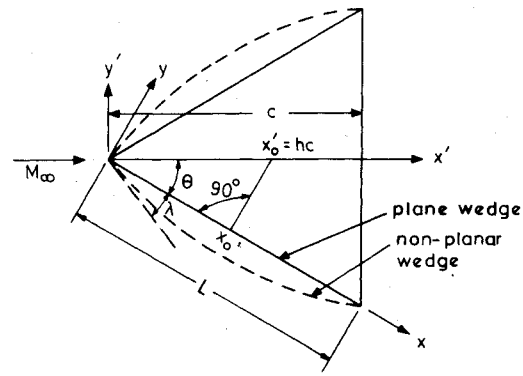

Fig. 1 b) Plane and nonplanar wedge; transfer of pivot position from x_0 to x_0'.

The similarity parameters can be shown to be $M_\infty\sin\alpha$ and $\phi M_\infty\cos\alpha$. However, for the flat plate case, the latter is not an independent parameter (since ϕ is wholly determined by M_∞, α, and r), but it is automatically satisfied if the former is satisfied, as shown below. From oblique shock relations, for $\phi\ll 1, \alpha\gg\phi$,

$$\phi/\tan\alpha=[(r-1)M_\infty^2\sin^2\alpha+2]/[(r+1)M_\infty^2\sin^2\alpha]$$

or

$$\phi M_\infty\cos\alpha=M_\infty\sin\alpha\cdot[(r-1)M_\infty^2\sin^2\alpha+2]$$
$$/[(r+1)M_\infty^2\sin^2\alpha]$$

But, for a nonplanar surface, for example, the biconvex airfoil ϕ is not determined by M_∞, r and α. Then, $\phi M_\infty\cos\alpha$ is an independent similarity parameter.

Received Nov. 30, 1978; revision received Jan. 28, 1980.

Index categories: Nonsteady Aerodynamics; Supersonic and Hypersonic Flow.

*Assistant Professor, Dept. of Aeronautical Engineering.

†Student in Master of Technology Program, Dept. of Aeronautical Engineering.

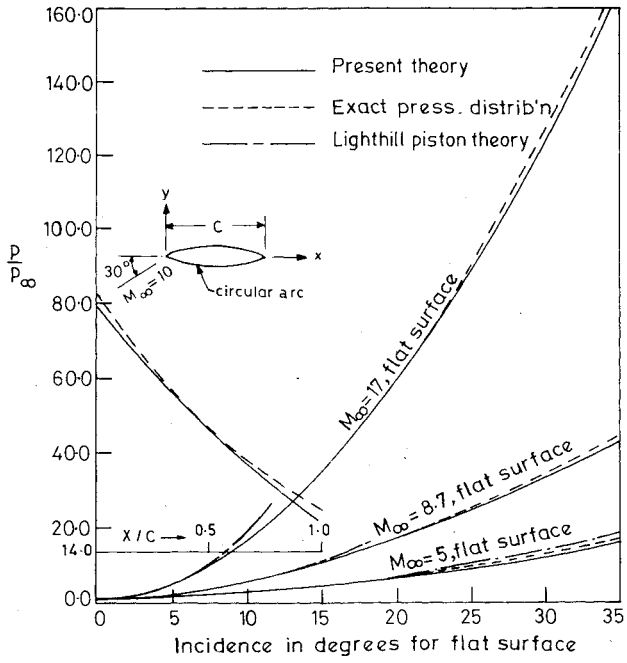

Fig. 2 Flat surface: pressure vs incidence, $r=1.4$; biconvex airfoil (semi-nose-angle 11.3 deg): pressure vs position, $\alpha=30$ deg, $r=1.4$.

Piston Theory

The airfoil geometry and motion gives piston velocity u_p, which is related to pressure p. Since the piston Mach number $M_p \equiv u_p/a_\infty \gg 1$, instead of the approximate expression of Lighthill,[2] the exact expression is used which can be written in quadratic form in pressure ratio, yielding

$$\frac{p}{p_\infty} = 1 + AM_p^2 + AM_p (B+M_p^2)^{1/2}$$

$$A = \frac{r(r+1)}{4} \qquad B = \left(\frac{4}{r+1}\right)^2 \ldots \tag{2}$$

Pressures on a steady flat plate and biconvex airfoil (semi-nose-angle 11.3 deg) have been calculated (Fig. 2). This theory has been applied for an oscillating plane wedge. The two surfaces of the wedge can be treated separately as flat plates (Fig. 1b). Consider the lower one oscillating about $x=x_0$. The nose down moment

$$-m = \int_0^L (x-x_0)p\,dx \ldots \tag{3}$$

The stiffness and damping derivatives are, respectively,

$$-C_{m_\alpha} = \frac{1}{\frac{1}{2}\rho_\infty U_\infty^2 L^2}\left(\frac{-\partial m}{\partial \alpha}\right), \quad -C_{m_{\dot\alpha}} = \frac{1}{\frac{1}{2}\rho_\infty U_\infty L^3}\left(-\frac{\partial m}{\partial \dot\alpha}\right)$$

evaluated at $\alpha=\theta$ and $\dot\alpha=0$. Piston Mach number

$$M_p = \frac{1}{a_\infty}\left[U_\infty \sin\alpha + (x-x_0)\dot\alpha\right] \ldots \tag{4}$$

By combining Eqs. (2-4), differentiation within the integral sign and integration are performed. Then, shifting axis of oscillation from x_0 to x_0' (Fig. 1b) and defining h as x_0'/c, $x_0 = hL\cos^2\theta$. Multiplying by 2 for effects of two sides and replacing L by C in nondimensionalizing, the derivatives of a plane wedge are

$$-C_{m_\alpha} = (r+1)(\tan\theta)(2+D+1/D)(\tfrac{1}{2}-h\cos^2\theta) \tag{5a}$$

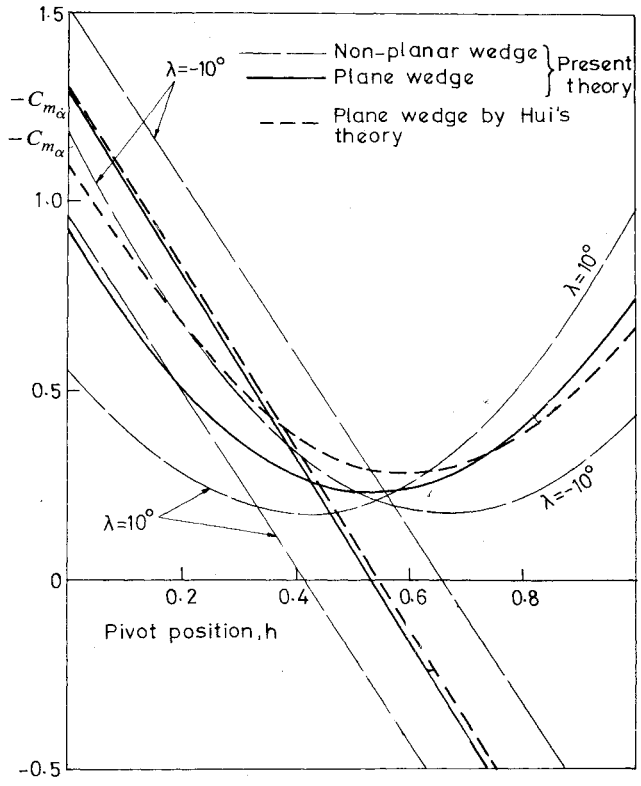

Fig. 3 Stiffness and damping derivatives of plane and nonplanar wedges, $M_\infty=10$, $\theta=15$ deg, $r=1.4$.

$$-C_{m_{\dot\alpha}} = (r+1)(\tan\theta/\cos^2\theta)(2+D+1/D) \times (1/3 - h\cos^2\theta + h^2\cos^4\theta) \tag{5b}$$

where

$$D = \left[\left(\frac{4}{\gamma+1}\right)^2 + M_\infty^2 \sin^2\theta\right]^{1/2} \Big/ (M_\infty \sin\theta)$$

Oscillating Nonplanar Wedge

A nonplanar wedge is obtained by superposing parabolic arcs on the two sides of the plane wedge (Fig. 1b). The slope of the lower parabolic arc, $dy/dx = \lambda(2\cdot x/L - 1)$, where $\lambda(\ll 1)$, is the slope at the leading edge.

$$M_p = \left[U_\infty \sin\alpha - U_\infty \cos\alpha \cdot dy/dx + (x-x_0)\dot\alpha\right]/a_\infty \ldots \tag{6}$$

Combining Eqs. (2), (3), and (6) and thereafter following the same process as in the case of a plane wedge, the aerodynamic derivatives are obtained.

$$-C_{m_\alpha} = \frac{(r+1)}{2M_\infty^2 \cos^2\theta}(I_1 + I_2 + I_3)$$

and

$$-C_{m_{\dot\alpha}} = \frac{(r+1)}{2M_\infty \cos^3\theta}(J_1 + J_2 + J_3)$$

where

$$I_1 = M_\infty^2 (H\sin 2\theta - (2\lambda\cos 2\theta)/3.0)$$

$$I_2 = [\{-M_\infty z^{3/2}/(3b)\}\{H\cos\theta + (H\lambda\sin\theta + \cos\theta) \times (5a-3z)/(5b) + \lambda\sin\theta(15z^2 - 42az + 35a^2)/(35b^2)\}]_{z=a+b}^{z=a-b}$$

$$I_3 = [\{M_\infty z^{1/2}/(2\lambda\cos\theta)\}\{-H\sin\theta\cos\theta$$

$$+ (z-3a)(\sin\theta\cos\theta - \lambda H(\cos^2\theta+\cos2\theta))/(3b)$$

$$+ (3z^2-10az+15a^2)(\cos^2\theta+\cos2\theta)\cdot\lambda/(15b^2)\}]_{z=a+b}^{z=a-b}$$

$$J_1 = M_\infty\sin\theta\cdot H^2 + M_\infty(\sin\theta - 2\lambda H\cos\theta)/3.0$$

$$J_2 = [\{-2z^{3/2}/(3b)\}\{H^2/4.0 + H(5a-3z)/(10b)$$

$$+ (15z^2-42az+35a^2)/(140b^2)\}]_{z=a+b}^{z=a-b}$$

$$J_3 = [\{-z^{1/2}/(\lambda\cos\theta)\}\{(H^2\sin\theta)/4.0$$

$$- H(\sin\theta - \lambda H\cos\theta)(z-3a)/(6b)$$

$$+ (\sin\theta - 4\lambda H\cos\theta)(3z^2-10az+15a^2)/(60b^2)$$

$$+ \lambda(5z^3-21z^2a+35za^2-35a^3)\cos\theta/(70b^3)\}]_{z=a+b}^{z=a-b}$$

In the preceding equations,

$H = 1 - 2h\cos^2\theta$, $a = [4/(r+1)]^2 + M_\infty^2\sin^2\theta$, and $b = \lambda M_\infty^2\sin2\theta$. Figure 3 compares results for plane wedge with Hui's theory and also with convex (λ positive) and concave (λ negative) nonplanar wedges.

Conclusion

Figure 2 demonstrates the theory's wide application range, in incidence and Mach number, for planar and nonplanar surfaces. It is free from the restrictions of Lighthill's[2] theory ($\alpha \ll 1$, $M_\infty\alpha \leq 1$) and Miles'[11] theory ($\alpha \ll 1$, $M_\infty\alpha \gg 1$). Figure 3 shows that the effect of convexity in nonplanar wedges is to decrease stiffness and shift damping minima towards the leading edge. Differences with Hui's theory for the plane wedge are attributed to neglect of secondary wave reflections in the present theory.

References

[1] Sychev, V. V., "Three Dimensional Hypersonic Gas Glow Past Slender Bodies at High Angles of Attack," *Journal of Applied Mathematics and Mechanics*, Vol. 24, Aug. 1960, pp. 296-306.

[2] Lighthill, M. J., "Oscillating Aerofoil at High Mach Numbers," *Journal of Aeronautical Sciences*, Vol. 20, June 1953, pp. 402-406.

[3] Appleton, J. P., "Aerodynamic Pitching Derivatives of a Wedge in Hypersonic Flow," *AIAA Journal*, Vol. 2, Nov. 1964, pp. 2034-2036.

[4] Orlik-Rückemann, K. J., "Effect of Wave Reflections on the Unsteady Hypersonic Flow over a Wedge," *AIAA Journal*, Vol. 4, Oct. 1966, pp. 1884-1886.

[5] McIntosh, S.C., Jr., "Studies in Unsteady Hypersonic Flow Theory," Ph.D. Dissertation, Stanford Univ., Calif., Aug. 1965.

[6] Hui, W. H., "Stability of Oscillating Wedges and Caret Wings in Hypersonic and Supersonic Flows," *AIAA Journal*, Vol. 7, Aug. 1969, pp. 1524-1530.

[7] Ericsson, L. E., "Viscous and Elastic Perturbation Effects on Hypersonic Unsteady Airfoil Aerodynamics," *AIAA Journal*, Vol. 15, Oct. 1977, pp. 1481-1490.

[8] Orlik-Rückemann, K. J., "Stabililty Derivatives of Sharp Wedges in Viscous Hypersonic Flow," *AIAA Journal*, Vol. 4, June 1966, pp. 1001-1007.

[9] Mandl, P., "Effect of Small Surface Curvature on Unsteady Hypersonic Flow over an Oscillating Thin Wedge," *C.A.S.I. Transactions*, Vol. 4, No. 1, March 1971, pp. 47-57; see also Errata in *C.A.S.I. Transactions*, Vol. 8, No. 2, 1975, p. 50.

[10] Ghosh, K., "A New Similitude for Aerofoils in Hypersonic Flow," *Proceedings of the 6th Canadian Congress of Applied Mechanics*, Vancouver, Canada, May 29-June 3, 1977, pp. 685-686.

[11] Miles, J. W., "Unsteady Flow at Hypersonic Speeds," *Hypersonic Flow*, Butterworths Scientific Publications, London, England, 1960, pp. 185-197.

J80-190

Flowfield Model for a Rectangular Planform Wing beyond Stall

00001
20016

Allen E. Winkelmann* and Jewel B. Barlow†
University of Maryland, College Park, Md.

Introduction

THE purpose of this Note is to propose a new, general flowfield model for the separated flow over a rectangular planform wing at subsonic speeds and high angles of attack. This model is consistent with earlier observations such as reported in Refs. 1-5, but is primarily inspired by new experimental studies at the University of Maryland. Oil flow studies by Winkelmann et al.[6] have shown strong counter-rotating swirl patterns to occur on reflection plane and full span "two-dimensional" rectangular wings with NACA 0015 and NACA 64_1A211 airfoils in the vicinity of stall. The results of more recent wind tunnel tests (to be reported in this Note) have also shown counter-rotating swirl patterns to exist on stalled finite wings which were free of any direct wall interference effects.

Experiment

Wind tunnel tests were conducted using a series of rectangular planform wings, all with the same 8.89-cm chord 14% Clark Y airfoil section. Primary interest was in the poststall behavior and flowfield. Three test series were completed: 1) a wing model with an aspect ratio $AR = 3.5$ was tested in the 0.46×1.17 m Aerospace Tunnel at a Reynolds number based on a chord of $Re_c = 245{,}000$; 2) a wing model with $AR = 2.86$ was tested in a 0.38×0.38 m student tunnel at $Re_c = 260{,}000$, and 3) a set of wing models with $AR = 3$, 6, 9, and 12 were tested in the 2.36×3.35 m Glenn L. Martin Tunnel at $Re_c = 385{,}000$. Photographs of surface oil flow patterns were obtained in all three cases. Lift, drag, and pitching moment data were taken during the first test series, and a number of exploratory flowfield studies were made during the second test series.

Results

Figure 1 shows a photograph of the oil flow patterns developed on the upper surface of the $AR = 3.5$ wing (test series 1) at an angle of attack $\alpha = 22.8$ deg. The lift coefficient at this point had already gradually rolled off from a maximum at 20.0 deg. A large region of reversed flow is apparent at the central portion of the wing. The oil flows into a pair of counter-rotating swirl patterns and collects in node points. The leading edge separation bubble is highly three-dimensional with the oil tending to form a characteristic "bead-like" pattern.

The "mushroom" shaped three-dimensional separation cell started to develop at $\alpha \simeq 18$ deg with the first signs of trailing edge separation occurring at $\alpha \simeq 15$ deg. The trailing edge stall cell grew in size until, at $\alpha = 26.1$ deg, the surface pattern abruptly changed and the three-dimensional separation line extended to the leading edge. This abrupt change was accompanied by a sudden loss of lift and a noticeable increase in wing buffeting. With increasing α, the counter-rotating swirl patterns were located near the wing tips and a uniformly reversed surface flow existed over most of the span.

Received Aug. 22, 1979; revision received Jan. 2, 1980.

Index categories: Subsonic Flow; Aerodynamics.

*Assistant Professor, Dept. of Aerospace Engineering. Member AIAA.

†Associate Professor and Director, Glenn L. Martin Wind Tunnel, Dept. of Aerospace Engineering. Member AIAA.